Article

pubs.acs.org/Biomac

Elastic and pH-Responsive Hybrid Interfaces Created with Engineered Resilin and Nanocellulose

Wenwen Fang,[†] Arja Paananen,[‡] Marika Vitikainen,[‡] Salla Koskela,[‡] Ann Westerholm-Parvinen,[‡] Jussi J. Joensuu,[‡] Christopher P. Landowski,[‡] Merja Penttilä,[‡] Markus B. Linder,[†] and Päivi Laaksonen*[,†]

[†]Department of Bioproducts and Biosystems, Aalto University, Espoo, FI-00076 Aalto, Finland

[‡]VTT Technical Research Centre of Finland Ltd., Espoo, FI-02044 VTT, Finland

Supporting Information

ABSTRACT: We investigated how a genetically engineered resilin fusion protein modifies cellulose surfaces. We characterized the pH-responsive behavior of a resilin-like polypeptide (RLP) having terminal cellulose binding modules (CBM) and showed its binding to cellulose nanofibrils (CNF). Characterization of the resilin fusion protein at different pHs revealed substantial conformational changes of the protein, which were observed as swelling and contraction of the protein layer bound to the nanocellulose surface. In addition, we showed that employment of the modified resilin in cellulose hydrogel and nanopaper increased their modulus of stiffness through a cross-linking effect.

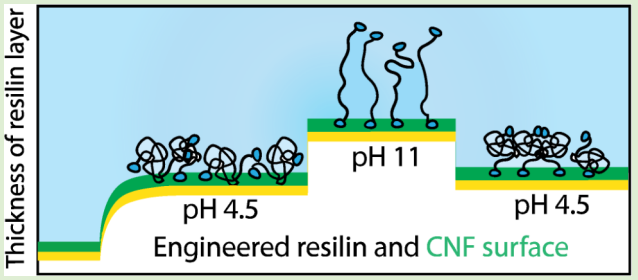

INTRODUCTION

In nature, biocomposites are often composed of stiff building blocks that are embedded in a matrix of softer materials. In such composite structures, the interfaces between the components carrying differing mechanical and chemical nature are in a key role for creating efficient transfer of mechanical stress, which has a major contribution in preventing damage through toughening of the materials.[1] Together with biomimetics, the present biosynthetic methods and advanced biorefinery offer possibilities for design of new materials combining great abilities of components.

Cellulose is the most abundant biopolymer in the biosphere and is found as hierarchical fibers in plants and sea animals acting as rigid building blocks, which heavily contribute to stiffness and strength.[2,3] Cellulose nanofibrils (CNF) are thin fibrils disintegrated from macroscopic pulp fibers by mechanical treatments, sometimes including pretreatment with chemicals and enzymes to help separating the fibrils. The CNF typically have a width of 5−20 nm and the length can be several micrometers. Due to their high aspect ratio, the CNF form entangled hydrogel-like structures.[4] Nanocelluloses have recently gained increasing attention because of their biodegradability, low cost, low density and good mechanical properties.[5] Particularly, CNF can be employed as a building block for nanocomposites of water-soluble components because it is well dispersed in water without any chemical modifications.

Resilin is an elastomeric protein found in specialized regions of the cuticle of most insects, for example, fleas, dragonflies, and spittle bugs.[6] It has outstanding elasticity and long fatigue life and is purported to be one of the most resilient elastic materials known.[7,8] The N-terminal domain of the *Drosophila melanogaster* CG15920 resilin protein, encoded by the first exon of the gene, consists of 18 copies of a 15-residue repeat consensus sequence (GGRPSDSYGAPGGGN).[7,9] This N-terminal domain, named Rec1-resilin, is the first recombinant resilin-mimetic polypeptide to be expressed and studied.[7] Recently, the secondary structure of Rec1-resilin was studied by Dutta et al. (2015) using circular dichroism (CD) spectroscopy and small-angle X-ray scattering (SAXS), and resilin was found to display equilibrium structural qualities between a structured globular protein and a denatured protein.[9] The high content of glycine and proline residues confers to resilin a high degree of flexibility and conformational disorder, which contributes to the mechanical properties of the protein.[10,11] Resilin also shows multistimuli responsiveness to thermal and pH changes in aqueous solution,[12] which have potential applications in creating patterned surfaces and responsive surfaces for uses in biosensors or diagnostic tools.[13] Truong et al. demonstrated that the conformational and viscoelastic properties of immobilized Rec1-resilin on the gold surface are switchable simply by changing the pH of the solution.[14]

In this study, we created cellulose/resilin hybrid materials to mimic bionanocomposite structures. Therefore, we used the soft and very elastic exon I region[11] of the Rec1-resilin from *Drosophila melanogaster* and the stiff but flexible cellulose nanofibrils as building blocks to make nanocomposites. To promote the interactions of CNF and resilin for realizing cellulose/resilin hybrid materials, cellulose binding modules (CBMs) were fused to the resilin-like polypeptide (RLP) at both C terminal and N terminal through genetic engineering

Received: February 27, 2017
Revised: April 24, 2017
Published: April 25, 2017

DOI: 10.1021/acs.biomac.7b00294
Biomacromolecules 2017, 18, 1866−1873

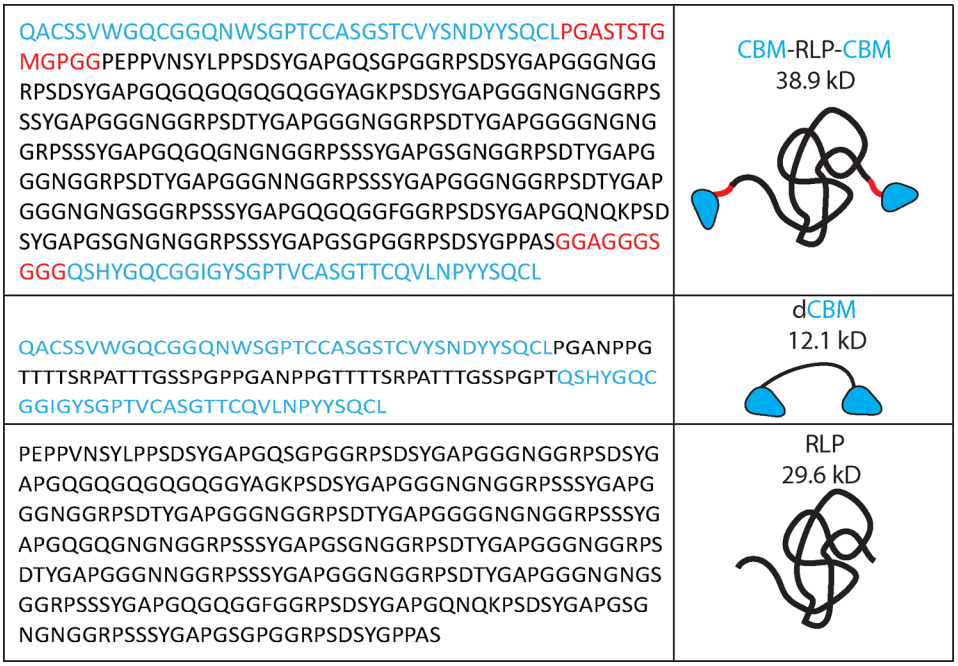

Figure 1. Amino acid sequences of CBM-RLP-CBM, RLP, and dCBM. Different colors of the sequence and the cartoon distinguish the cellulose binding modules (blue), the linker (red), and the resilin-like polypeptide (black).

(Figure 1). The resulted fusion protein is referred to as the CBM-RLP-CBM. The chosen CBMs are the noncatalytic domains of the cellobiohydrolase enzyme, which bring the catalytic part of the cellulase close to the surface.[15,16] The fungal CBMs (from family I) employed here bind to cellulose crystals through a set of aromatic residues and hydrogen bonding.[17] According to the previous reports, functionalization of cellulose nanocrystals (CNC) with CBMs and their fusion proteins has been carried out successfully and shown to affect their colloidal properties and the mechanical properties of materials derived from the CNC.[18,19] Here, CBM-RLP-CBM and its behavior on the surface of cellulose nanofibrils were studied at different pHs. Finally, we formed cellulose/resilin hydrogels and nanocomposites to understand how the protein acts as a CNF cross-linker and how the surface-bound resilin contributes to their mechanical properties of such hybrid materials.

MATERIALS AND METHODS

Production of Cellulose Nanofibrils. Cellulose nanofibrils (CNF) were prepared by fluidizing never-dried fully bleached sulfite hardwood (Birch) pulp obtained from a Finnish pulp mill (kappa number 1; DP 4700; fines removed (SCAN-M 6:69)). The pulp was washed to the sodium form according to Swerin et al. to control both the counterion type and ionic strength.[20] The washed pulp was disintegrated by passing through a high-pressure fluidizer (Microfluidics M110P, Microfluidics Int. Co., Newton, MA) for six times. No chemical or enzymatic pretreatment was used prior to disintegration.

Construction of Resilin Expression Plasmids and *T. reesei* Strains. Synthetic genes encoding the Rec1-resilin (RLP) and Rec1-resilin flanked with CBMs (CBM-RLP-CBM) were codon optimized for *Trichoderma reesei* and synthesized. The *T. reesei* CBHII (cellobiohydrolase II; Cel6A) CBM is placed at the N-terminus and the *T. reesei* CBHI (cellobiohydrolase I; Cel7a) CBM at the C-terminus of the CBM-RLP-CBM construct (Figure 1). An N-terminal eight histidine-tag and a C-terminal Strep tag (WSHPQFEK) were added to the proteins to enable affinity purification. The synthetic gene fragments were cloned into expression plasmids containing *cbh1* promoter, secretion carrier and terminator, hygromycin selection marker, and targeting sequence for the *cbh1* locus. The RLP and CBM-RLP-CBM were expressed as CBHI carrier protein fusions with a KEX2 protease cleavage site, NVISKR, between the carrier and the RLP or CBM-RLP-CBM protein (Figure S1, Supporting Information).[21] The RLP construct (pHYB49) was cloned by Golden gate cloning[22] into a destination plasmid, pJJJ395, using the BsaI restriction enzyme. The ligation product was transformed to Top10 *E. coli* cells and selected on kanamycin plates by blue-white screening to identify clones containing the insert. The CBM-RLP-CBM construct (pAWP116) was cloned by yeast homologous recombination[23] into the pTTv248 expression plasmid, together with CBHI carrier fragment. After plasmid rescue from yeast the plasmid was transformed into Top10 *E. coli* cells and selected on ampicillin plates. The correct assembly of the RLP (pHYB49) and CBM-RLP-CBM (pAWP116) plasmids were verified by restriction enzyme analysis and by DNA sequencing. The transformation cassettes were cut from the vectors with PmeI restriction enzyme and purified from agarose gel. The cassettes were transformed to protease deficient *Trichoderma reesei* strains[24] essentially as described[25] and were selected for hygromycin resistance on plates containing 125 μg/mL of hygromycin B. Transformant were screened by PCR for correct integration of the constructs to the *cbh1* locus (Table S1, Supporting Information). The final strains were designated RLP and CBM-RLP-CBM.

Production of the proteins. *Trichoderma reesei* strains expressing the CBM-RLP-CBM (M1438) or the RLP (M1912) protein were grown in 24 well plates in TrMM plus 40 g/L lactose, 20 g/L spent grain extract, 8.6 g/L diammonium citrate, 5.4 g/L $NaSO_4$, 100 mM PIPPS at pH 4.5, shaking at 28 °C at 800 rpm (Infors AG). TrMM contains 15.0 g/L KH_2PO_4, 2.4 mM $MgSO_4{\cdot}7H_2O$, 4.1 mM $CaCl_2{\cdot}H_2O$, 3.7 mg/L $CoCl_2$, 5 mg/L $FeSO_4{\cdot}7H_2O$, 1.4 mg/L $ZnSO_4{\cdot}7H_2O$, and 1.6 mg/L $MnSO_4{\cdot}7H_2O$. The *T. reesei* fungus secreted the CBM-RLP-CBM and RLP proteins into the culture medium. A total of 1 L of culture was grown for 5 days in 24-well plates (5 mL per well in multiple plates). The growth medium was filtered through a glass-microfiber filter to remove the mycelium and 0.5 mM phenylmethylsulfonyl fluoride (PMSF) was added to the clarified culture supernatant for stabilization. The reference protein dCBM was produced by linker digestion of hydrophobin (HFB)-dCBM with trypsin.[26]

Purification of the Proteins. The RLP and CBM-RLP-CBM contained a polyhistidine tag, which allowed purification by

DOI: 10.1021/acs.biomac.7b00294
Biomacromolecules 2017, 18, 1866−1873

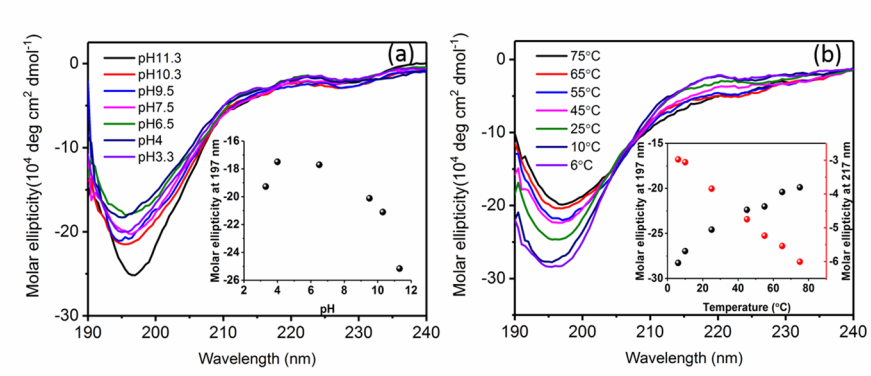

Figure 2. Far-UV CD spectra of CBM-RLP-CBM at different pHs (a) and different temperatures (b). The inset in (a) is the molar ellipticity at 197 nm vs pH, and the inset in (b) is the molar ellipticity at 197 and 217 nm vs temperature. The 6 μM protein water solution was used for the CD measurement and the pH was adjusted with HCl and NaOH.

immobilized metal chelating chromatography (IMAC). Filtered culture supernatant was loaded on chelating sepharose FF (GE Healthcare, U.K.), previously equilibrated with 20 mM sodium phosphate buffer, pH 7.4, containing 500 mM NaCl and 10 mM imidazole. Elution was performed using 500 mM imidazole. The fractions of the IMAC run were analyzed by SDS−PAGE (Gel Code Blue Stain, Pierce) and after blotting to nitrocellulose filters, by Western blotting. The membrane was blocked with 5% nonfat milk in TBST buffer (50 mM Tris, 150 mM NaCl, 0.05% Tween, pH 7.4) and then probed with streptactin-AP 35 conjugate (1:2000 in TBST, IBA Gmbh) and chromogenic detection with NBT/BCIP (Promega). The pooled protein sample was gel filtrated on a Bio-Gel P6DG (Bio-Rad) column to DDIW as a final purification step. The peak fractions were pooled and lyophilized. The amino acid sequences of CBM-RLP-CBM and dCBM are shown in Figure 1. The protein construct has two different CBM units CBM_{CBHI} and CBM_{CBHII}.[27]

Characterization of the Protein with Circular Dichroism Spectroscopy. The circular dichroism (CD) spectra of CBM-RLP-CBM were measured with a Chirascan CD spectrophotometer (Applied Photophysics, Leatherhead, U.K.) at different pH values and temperatures. The pH value of the CBM-RLP-CBM solution was adjusted with NaOH and HCl. The temperature was controlled by placing a thermoprobe connected with a temperature control set into the measuring cell. The CD spectra were recorded using a 1 mm cell and bandwidth of 1 nm from 240 to 190 nm UV light. The data is expressed in terms of molar ellipticity in deg·cm^2 dmol^{-1}.

Characterization of the Protein by ζ-Potential Measurements. The ζ-potential of the CBM-RLP-CBM at different pHs was measured by a particle analyzer instrument (Zetasizer Nano ZS, Malvern, U.K.) to determine the isoeletric point (IEP) of the protein. The pH of the CBM-RLP-CBM solution was adjusted by HCl and NaOH. The concentration of the protein solution was chosen to be 0.1 g L^{-1} to avoid multiple scattering.

Characterization of the Protein Films by Quartz Crystal Microbalance. Adsorption of the proteins on nanocelullose and the behavior of the hybrid films were characterized by quartz crystal microbalance with dissipation monitoring (QCM-D). The gold-coated quartz crystal sensors with fundamental frequency near 5 MHz were cleaned with piranha solution. The cleaned quartz crystals were then coated with CNF using a spin-coater (Model WS-650SX-6NPP, PA, U.S.A.) to prepare cellulose thin films. For spin-coating, a 0.01% water suspension of CNF was applied at 3500 rpm spinning rate.

The QCM-D experiments were performed using a Q Sense E4 instrument (Biolin Scientific, Sweden). The changes in resonance frequency, f, and dissipation, D, were recorded. For a rigid film, the adsorbed mass can be estimated from the change of the resonant frequency Δf by using the Sauerbrey equation:

$$\Delta m = -\frac{C\Delta f}{n}$$

where C (17.7 ng cm^{-2} Hz^{1-} at f_0 = 5 MHz) is the mass sensitivity constant and n is the overtone number. The Sauerbrey equation is valid for rigid, evenly distributed, and sufficiently thin adsorbed films. In soft adsorbed films that differ significantly from the underlying sensor surface by their viscoelasticity, the Sauerbrey relation underestimates the adsorbed mass because the propagation of the shear acoustic wave in the adsorbed layer does not follow the shear oscillation of the sensor crystal. The Sauerbrey equation was employed for estimating the indicative number of molecules adhered to the surface. Under the conditions of the nonrigid films, the Voigt viscoelastic model was used to estimate the thickness of the film. The QCM-D measurements were performed under a continuous flow rate of 0.1 mL min^{-1} with a protein concentration of 0.1 mg mL^{-1}. The protein was dissolved in 10 mM acetic acid buffer at different pHs. At least two parallel runs were carried out for each experiment.

Characterization of the Rheology of the Hybrid Hydrogels. Rheological measurements of ultrasonicated nanocellulose-protein mixtures (2 mg mL^{-1} CNF, 0−80% protein CBM-RLP-CBM of the amount of CNF in water) were carried out at room temperature (22 °C) with a rheometer (AR-G2, TA Instruments, Delaware, U.S.A.) equipped with plate−plate geometry. The diameter of the plates was 20 mm. The viscoelastic properties of the CNF-protein mixtures were determined in small deformation oscillation mode of the rheometer using a sample volume of 350 μL and a 1 mm gap. Time sweep (frequency 0.1 Hz, strain 1%; linear region) was run for 2 h, followed by amplitude and frequency sweeps. Evaporation of the sample was prevented by sealing the sample with oil.

Preparation of Hybrid Films. The desired proportions of CNF/CBM-RLP-CBM dispersions were prepared by tip sonication at a 20% amplitude for 1 min using a Branson sonifier (Emerson Electric, U.S.A.) with a 1/8″ microtip. The CNF concentration was kept at 2 g L^{-1} throughout the experiments. The CNF/CBM-RLP-CBM films were prepared from the suspensions through vacuum filtration using a Durapore membrane (GVWP, 0.22 μm, Millipore, U.S.A.). The films were dried at ambient conditions.

Tensile Tests of the Hydrid Films. The films were equilibrated at 50 or 80% relative humidity and stored at 20 °C overnight before the tensile testing. The mechanical properties were measured in a custom-made humidity chamber using a tensile tester (Tensile/Compression Module 5 kN with a 100 N load cell, Kammrath & Weiss GmbH). The rate of elongation was set at 0.5 mm min^{-1} and the gauge length was 10 mm. Specimen sizes were 20 × 2 mm (length and width, respectively). The thickness of the films was measured using a film thickness measurement setup, composed of a displacement sensor (LGF-0110L-B, Mitutoyo), digital reader (EH-10P, Mitutoyo), and a measuring table with support for sensor (215−514 comparator stand, Mitutoyo). At least five specimens were measured for each sample. The Young's modulus, yield stress and strain, and ultimate stress and strain were calculated from the average of strain−stress curves with Matlab. The significant change of the slope in the strain−stress curves

DOI: 10.1021/acs.biomac.7b00294
Biomacromolecules 2017, 18, 1866−1873

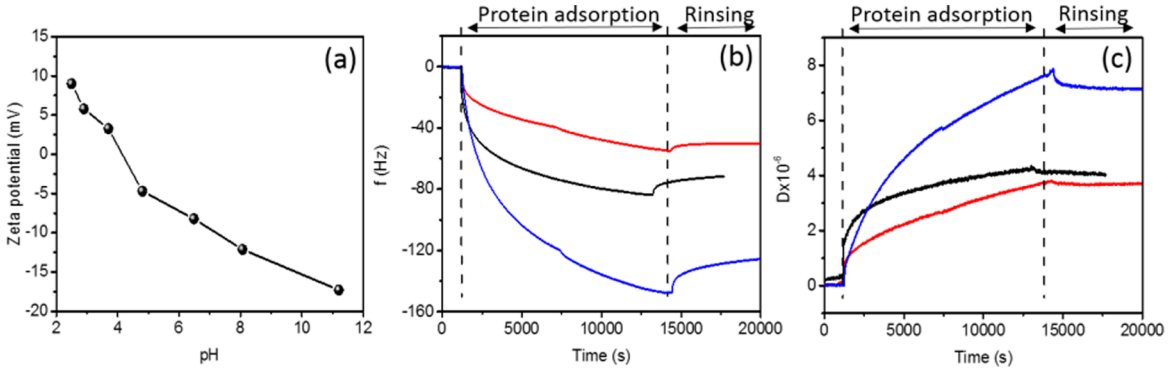

Figure 3. (a) ζ-Potential of CBM-RLP-CBM at different pH values. QCM-D adsorption curves showing the shift in resonance frequency (b) and dissipation (c) at n = 5, as CBM-RLP-CBM is adsorbed onto the CNF coated gold substrate at pH 3 (blue), 4.5 (black), and 8 (red).

is named as yield point. The stress and strain at the yield point are defined as yield stress and strain, respectively.

RESULTS AND DISCUSSION

Characterization of CBM-RLP-CBM at Different pH. In order to investigate the secondary structure of the CBM-RLP-CBM, protein solutions at different pH values were examined with CD spectroscopy. The spectra as a function of pH are shown in Figure 2a. At the isoelectric point (IEP; pH close to 4.5 as discussed in the later section), the CD spectrum displayed a large negative band at wavelength 195−200 nm and a low ellipticity above 210 nm. When varying the pH to values significantly lower or higher than the IEP, a clear reduction in the ellipticity was observed. However, the shape of the CD spectra was very similar in all of the pHs, indicating that there were no substantial changes in the secondary structure. At pH 11.4, the large band was slightly shifted toward higher wavelengths.

The negative band at 195−200 nm suggested the presence of random coil conformers predominant in the CBM-RLP-CBM, which is in accordance with earlier observation that the secondary structure of resilin is largely disordered.[9] The typical poly-L-proline type II (PPII) helix CD spectra are characterized by a strong negative band at 195−200 nm and a weak positive band at 217 nm.[28] The negative band becomes less intense as the temperature increases.[29] By measuring the CD spectra of resilin at different temperatures (Figure 2b), we found that there is a progressive increase of negative ellipticity values at 197 nm from 6 to 75 °C, together with a reduction of the negative band at 217 nm, which indicates the transformation of random coils to PPII structure at lower temperature.[30] The isoelliptic point near 208 nm in the temperature-dependent spectra (Figure 2b) also indicates a conformational equilibrium between the PPII structure and random coils.[28] The changes in the CD spectra as a function of pH may arise because of the changes of surface charges without any predictable secondary structural changes.

Adsorption of CBM-RLP-CBM on CNF. The ζ-potential of the protein at different pHs was measured to find out the effective isoelectric point (IEP) of the protein (Figure 3a). The ζ-potential is related to the charge of the particle near its surface, thus it is a good qualitative estimate of the exposed charge of the particle. The experimental isoelectric point IEP was estimated by interpolating the measured ζ-potential to zero and was near 4.5. However, the theoretical IEP value based on the peptide sequence is 7.9. The great difference between the theoretical and measured values indicates that a large fraction of the positively charged residues of the protein are not exposed to the surface, but embedded within the folded center of the protein. Dutta et al. proposed a core−shell structure for the resilin protein, where negatively charged amino acid residues are exposed to water and positively charged residues form the core, which is in perfect alignment with our observation.[12]

Adsorption of the CBM-RLP-CBM on the nanocellulose surface was studied using QCM-D by allowing the protein to adsorb at different pHs. The changes in the resonance frequency (Δf), and dissipation (ΔD) as a function of time during the adsorption of the CBM-RLP-CBM on the CNF surfaces at different pH values are presented in Figure 3b,c. The experimental pH values were chosen so that the protein would have negative (pH 8), neutral (pH 4.5), and positive surface charge (pH 3) to be able to observe the significance of the electrostatic interaction in the adsorption on the slightly negatively charged CNF layer.[31] Binding of the native fungal CBMs to cellulose is not very sensitive to pH and occurs as well at low and high pH values.[32] The significant decrease of the resonance frequency after injecting the protein shows that the CBM-RLP-CBM adsorbed to cellulose (Figure 3). Rinsing with the buffer could remove only a small fraction of the adsorbed protein. It was clear that the adsorption of the CBM-RLP-CBM on CNF was pH-dependent, which means that the electrostatics played a role in the binding, most likely due to the electrostatic attraction or repulsion between resilin and the CNF. According to earlier studies by Truong et al. that were carried out at different surfaces, the surface-bound Rec-1 resilin layer had also pH responsive behavior.[14]

At all the pH values, a rapid decrease of frequency at the early stage of adsorption was observed, followed by a steady gradual decrease toward a stable value. The response of plain CNF surface was much less pronounced (see Figure S2). The rate of the adsorption and the final value of mass depended on the pH, the lowest pH showing the highest bound mass, which is in accordance with the measured ζ-potentials, meaning that the stronger electrostatic attraction leads to higher amount of protein on the surface. The adsorption of the CBM-RLP-CBM on the cellulose surfaces was quite irreversible because only a small degree of desorption was observed after rinsing with buffer solutions. The protein packing density on the CNF surface estimated by the Sauerbrey mass was 2334 ng cm^{-2} at pH 3, 1317 ng cm^{-2} at pH 4.5 (IEP), and 999 ng cm^{-2} at pH 8. The Sauerbrey estimation allows calculation of the area occupied by a single molecule, which was 2.6, 5.0, and 6.1 nm^2 at pH 3, 4.5, and 8.0, respectively. The expected size of the CBM is near 4 nm^2, which indicates the formation of very

DOI: 10.1021/acs.biomac.7b00294
Biomacromolecules 2017, 18, 1866−1873

closely packed protein monolayers. We do not suggest formation of multilayers because the structure of the protein does not facilitate multimerization and the QCM-D mass includes also the mass of solvent associated with the proteins, which can form a substantial fraction of the total mass of the layer, thus, overestimating the actual mass of the proteins. Also, the nanoscale roughness of the nanocellulose increases the actual surface area, which makes the assumption of a monolayer feasible.

The saturation of the adsorbed amount of the proteins on the CNF surfaces appears very slow after a fast initial binding. One reason for the slow buildup of the protein mass can be the slight swelling of the CNF film due to the adsorbed proteins. This may lead to the increase of the porosity with time, meaning that the accessible surface area slowly increased as a function of time. It may also be that the proteins entanglement and orientation in the film slowly changed and allowed more proteins to bind.

Response of the Immobilized CBM-RLP-CBM to pH. In order to understand the conformational changes of the resilin, we studied how the CBM-RLP-CBM layer immobilized on the cellulose film responded to the pH changes. The thickness of the immobilized protein layer was calculated from the measured frequency and dissipation values by the Voigt model (Figure S2) assuming the density of 1200 g m^{-3} for the protein (Figure 4). In the experiment, the CBM-RLP-CBM

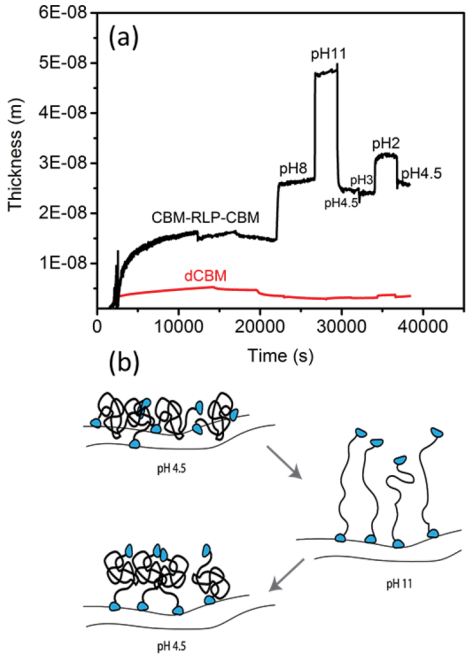

Figure 4. (a) Calculated thickness of immobilized CBM-RLP-CBM and dCBM layer formed at pH 4.5 and exposed to various pH values. (b) Schematic presentation of the conformation changing of CBM-RLP-CBM molecule at different pHs during QCM-D measurements.

was first immobilized on the CNF layer and stabilized at pH 4.5 (IEP), where it formed a 15 nm thick layer, which rather well corresponded to the estimated size of the CBM-RLP-CBM protein (Table S2). After stabilization of the layer, 10 mM citric buffer at different pH values was introduced to the measurement chamber. When exposed to pH 8, the thickness of the protein layer expanded to ~25 nm and at pH 11 to 50 nm. After swelling, the protein layer was contracted to a thickness below 25 nm by changing the pH to 4.5. Lowering the pH further to 3 did not change the layer thickness, but at pH 2 the layer swelled again. Finally, the pH was returned to the IEP, and the final layer thickness was near 25 nm, a higher value from the original thickness. As reference molecules, a smaller cellulose binding protein construct dCBM, having only two CBMs attached together through a simple peptide linker, and RLP without the CBMs were used, and as a reference surface, an unmodified CNF surface was used (Figures 4 and S2).

The CBM-RLP-CBM construct is asymmetric, because the CBMs are CBM_{CBHI} and CBM_{CBHII} and have different binding stability. The binding of the CBM_{CBHI} has been reported reversible by dilution, while the CBM_{CBHII} cannot be easily dissociated from cellulose by buffer dilution.[33] As a possible explanation for the irreversible changes in the film thickness after exposure to pH 11, we propose that the CBM_{CBHI} modules were desorbed from the surface at these conditions. As shown in the schematic in Figure 4, one of the terminal CBMs may have dissociated from the cellulose surface at pH 11, where the extension of the RLP was also observed. Returning the pH to value 4.5, probably lead to refolding of the RLP back to its original conformation, but due to the steric hindrance, the dissociated CBM could not fully bind to the surface again leaving the thickness of the protein layer higher than originally.

The thickness of the control dCBM layer at pH 4.5 was around 5 nm, which rather well corresponded to the estimated size of the dCBM (see Table S3), and there was only a slight decrease of thickness with changing of pH indicating the partial desorption of the protein. The CNF reference surface was significantly affected by the pH changes only at pH 11, where its mass apparently increased due to the impregnation of the buffer (Figure S2). Therefore, the majority of the changes in the film thickness were associated with changes in the proteins' conformation and electrostatics. The RLP protein without CBMs was used as reference and the results are shown in Figure S3 (Supporting Information). There was a certain amount of RLP adsorbed on the cellulose surface, but a large fraction desorbed when the surface was rinsed with the buffer. This observation indicated to a nonspecific binding of the reference protein, and confirmed that the adsorption of the CBM-RLP-CBM to cellulose occurred mainly through the CBMs. The original thickness of the RLP layer was around 18 nm, which is very close to the CBM-RLP-CBM layer, indicating their conformations were similar.

At pH 8 and 11 and at pH 2, the surface-bound resilin fusion protein was in the swollen conformation. The conformational changes were also observed in the CD spectra of the free protein. When comparing the responsiveness of the CBM-RLP-CBM and dCBM to pH, we can conclude that the pH-responsive properties of CBM-RLP-CBM mostly come from the resilin part, either due to the electrostatic interactions with the CNF surface or due to the conformational changes of resilin. At pH 4.5, the binding capacity estimated from the Sauerbrey mass of CBM-RLP-CBM on CNF was 0.035 nmol cm^{-2} and 0.065 nmol cm^{-2} for the dCBM. The adhered molar quantity of the smaller control protein having no resilin domain was expectedly higher because the resilin can spread on the surface and therefore occupies larger surface area allowing less proteins to bind.

To understand better the robustness of the pH-responsiveness of the CBM-RLP-CBM immobilized on the CNF surface, the resilin layer was adsorbed on the CNF and then exposed to

DOI: 10.1021/acs.biomac.7b00294
Biomacromolecules 2017, 18, 1866−1873

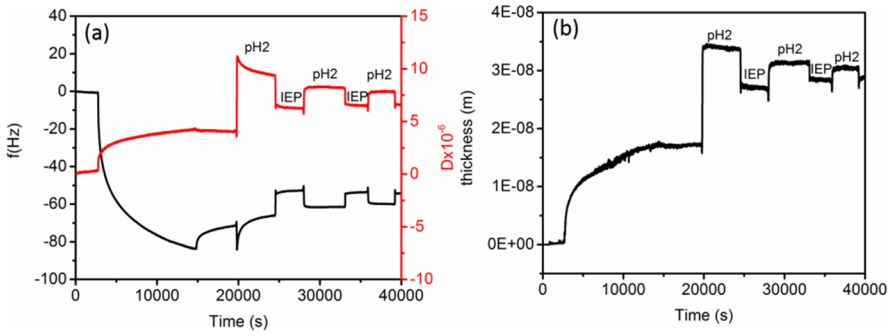

Figure 5. Response of the immobilized CBM-RLP-CBM to pH changes between pH 4.5 and pH 2 (a) and the estimated thickness based on the Voigt model (b).

buffers having pH 4.5 and pH 2 repeatedly. The resulting film thickness is presented in Figure 5 showing consequent changes in the film thickness. Introduction of the pH 2 buffer caused a rapid change in the frequency in the first cycle, leading to some desorption of the proteins. At the same time, an irreversible change in the thickness was observed, again probably due to the desorption of the CBM_{CBHI} module due to a sudden pH change leaving the thickness to higher value than originally. In the subsequent cycles, there was no clear indication of further desorption and the CBM-RLP-CBM responded to pH 2 and then recovered back to the original conformation once pH 4.5 buffer was introduced.

Rheology of the CNF/Resilin Hydrogels. Shear rheology of the CNF hydrogel and its combination with different amounts of the CBM-RLP-CBM protein were studied to understand how they interact in the liquid environment. The pure CNF solution was very fluidic and the measured storage modulus had a very low value (Figure 6). The viscoelastic

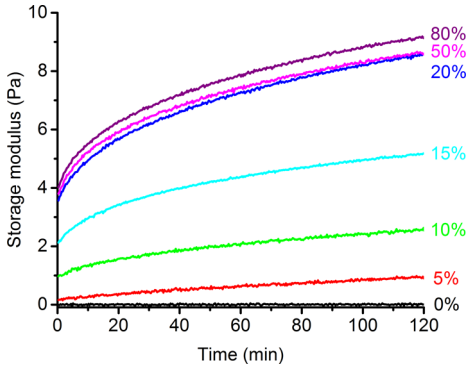

Figure 6. Shear storage modulus of the CNF-protein mixtures at different CBM-RLP-CBM concentrations. The percentage describes the amount of protein in relation to CNF. The CNF concentration is 2 g/L in all measurements.

moduli of the CNF/CBM-RLP-CBM mixtures increased steadily with increasing concentration of the CBM-RLP-CBM and saturated when the mass of the protein was 20% compared to the mass of CNF, since there was only a slight increase in the storage modulus when the protein concentration was increased from 20 to 80 wt % of CNF.

The increase of the storage modulus was due to the increased interaction between the CNF fibrils caused by the presence of the CBM-RLP-CBM. Since both the termini of the protein are capable of binding to the CNF, we propose that the protein cross-links the CNF network. In addition, there might be some entanglement of the RLP domains, which may also affect the elasticity and strength of the hydrogel. The saturation of the storage modulus value was related to the fact that the protein acts on the cellulose surfaces and was in accordance with some previous observations on binding of the double CBMs on CNF.[26,34]

Mechanical Properties of the CNF/CBM-RLP-CBM Hybrid Nanopapers. Tensile tests of the CNF nanopaper films with different amounts of CBM-RLP-CBM were carried out at 50% (Figure S4) and 80% relative humidity (RH; Figure 7). In all conditions, a pristine CNF film without protein additive was used as a control. At both 50% and 80% RH, addition of the CBM-RLP-CBM increased the stiffness and the yield stress of the samples, but had no clear improvement on their total strength or strain-to-failure. At 80% RH, CNF was generally softer than at 50% RH and the Young's modulus (YM) of the CNF film dropped from 7.8 to 4.5 GPa. However, the maximum strain of the CNF films increased from 12.5% to 17% at a higher humidity because of the plasticization by water. The effect of the humidity on the tensile properties of the CNF films has been studied in a previous study where similar findings were reported.[35] In the case of the resilin, the behavior of the materials at elevated humidity was especially interesting because of the high elasticity that resilin exhibits in humid conditions.[36] The RLP without the CBMs was used as a reference protein and the mechanical properties measured at 50% RH (Figure S4, Supporting Information). The CNF/RLP film had very similar properties compared to the CNF, and its yield stress was much lower than that of the CNF/CBM-RLP-CBM film, confirming that the CBMs were able to cross-link the fibrils.

At 80% RH, introduction of 20 wt % of the CBM-RLP-CBM increased the YM of the CNF films from 4.4 to 6.2 GPa. Above 20 wt % addition of the protein, the YM increased steadily with increasing protein concentrations and saturated at 80 wt %. The yield stress of the CNF films started to increase at a higher CBM-RLP-CBM dosage (above 50%) and kept increasing linearly the whole range of protein fractions. The strain decreased steadily with increasing protein addition, which indicates that the CNF films became stiffer but more brittle due to the cross-linkage via CBM-RLP-CBM. A similar phenomenon has been found in previous studies with dCBM.[26] Beyond the yield point, there was a clear strain hardening in the plastic deformation part of the pristine CNF sample, suggested by some fibril orientation during the deformation. Especially at high humidity conditions, there are more water molecules that compete with interfibril hydrogen bonding and, therefore, allow fibrils to slip more easily past each other. With 20 wt % of

DOI: 10.1021/acs.biomac.7b00294
Biomacromolecules 2017, 18, 1866−1873

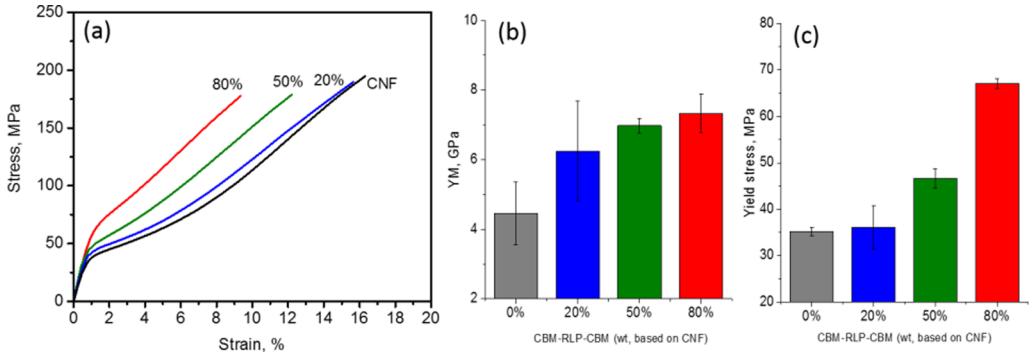

Figure 7. Tensile strain−stress curves of CNF and CBM-RLP-CBM nanocomposites at 80% RH (a) and the Young's modulus and yield stress are shown in (b) and (c), respectively: Unmodified CNF film (black), CNF film with 20% CBM-RLP-CBM (blue), CNF film with 50% (green), CNF film with 80% CBM-RLP-CBM (red). The error bars are the standard deviation of at least five repeated experiments.

CBM-RLP-CBM, there is still a slight strain stiffening, but afterward, tno strain stiffening was observed. This indicates that the CBM-RLP-CBM cross-linking prevented the sliding of the CNF fibrils, which lessened the ductility of the material.

For obtaining reliable tensile test data, the hydrogel samples needed to be very homogeneous with no aggregation. This set some limitation to the sample preparation conditions, and therefore, the effect of the pH and the related conformational changes of the protein could not be captured in these experiments. The main difficulties in adjusting the pH were the instability of the hydrogels either due to the electrostatic interactions between the proteins and the CNF or due to the sensitivity of the CNF to increased ionic strength. Adjusting the pH below the IEP of the protein led to fast aggregation of the hydrogels, whereas adjustment of the pH to higher than the IEP led to aggregation of the CNF alone.

CONCLUSIONS

A very elastic cellulose binding fusion protein and its interaction with nanocellulose was investigated. Two terminal cellulose binding domains were fused to a Rec1 resilin exon to create a cellulose binding resilin. Attachment of the protein via CBMs to the surface of nanocellulose films was confirmed. It was also shown that the elasticity and pH responsive behavior of the resilin was maintained at the surface-bound state. When embedded as a cross-linker in the CNF matrix, the resilin fusion protein increased the rigidity of the CNF network both in a hydrogel form and in the dried cellulose nanopapers. Surprisingly enough, the resilin did not soften the nanocellulose materials, but its main contribution was in increasing the stiffness and yield strength. In comparison, Rec1-resilin without the CBMs was embedded into the nanopaper but it did not change the properties when compared with pure CNF. The main conclusion of the work was that the resilin-like behavior was transferred into a fusion protein. The fusion protein was able to bind to cellulose, cross-link cellulose nanofibrils, and modify the interactions between the cellulose nanofibrils.

ASSOCIATED CONTENT

Supporting Information

The Supporting Information is available free of charge on the ACS Publications website at DOI: 10.1021/acs.biomac.7b00294.

QCM measurements of CNF reference surface, DCBM and CBM-RLP-CBM layer formed at pH 4.5 and exposed to different pHs, the sizes of proteins estimated by calculating the radius of gyration based on the protein sequence, tensile tests of the nanopapers with engineered resilin proteins (PDF).

AUTHOR INFORMATION

Corresponding Author

*E-mail: paivi.laaksonen@aalto.fi.

ORCID

Päivi Laaksonen: 0000-0003-2029-5275

Author Contributions

The manuscript was written through contributions of all authors. All authors have given approval to the final version of the manuscript.

Notes

The authors declare no competing financial interest.

ACKNOWLEDGMENTS

The authors acknowledge the Academy of Finland Center of Excellence Program, especially the Center of Excellence in Molecular Engineering of Biosynthetic Hybrid Materials (HYBER). Riitta Suihkonen is thanked for the technical assistance in the protein purification. Ilari Filpponen is thanked for the preparation of the cellulose nanofibrils. Sanni Voutilainen is acknowledged for the help with the CD spectrometer.

REFERENCES

(1) Laaksonen, P.; Szilvay, G. R.; Linder, M. B. *Trends Biotechnol.* **2012**, *30* (4), 191−196.

(2) Eichhorn, S. J.; Dufresne, A.; Aranguren, M.; Marcovich, N. E.; Capadona, J. R.; Rowan, S. J.; Weder, C.; Thielemans, W.; Roman, M.; Renneckar, S.; Gindl, W.; Veigel, S.; Keckes, J.; Yano, H.; Abe, K.; Nogi, M.; Nakagaito, A. N.; Mangalam, A.; Simonsen, J.; Benight, A. S.; Bismarck, A.; Berglund, L. A.; Peijs, T. *J. Mater. Sci.* **2010**, *45* (1), 1−33.

(3) Capadona, J. R.; Shanmuganathan, K.; Tyler, D. J.; Rowan, S. J.; Weder, C. *Science* **2008**, *319* (5868), 1370−1374.

(4) Klemm, D.; Kramer, F.; Moritz, S.; Lindström, T.; Ankerfors, M.; Gray, D.; Dorris, A. *Angew. Chem., Int. Ed.* **2011**, *50* (24), 5438−5466.

(5) Nishino, T.; Takano, K.; Nakamae, K. *J. Polym. Sci., Part B: Polym. Phys.* **1995**, *33* (11), 1647−1651.

(6) Weis-Fogh, T. *J. Exp. Biol.* **1960**, *37* (4), 889−907.

(7) Elvin, C. M.; Carr, A. G.; Huson, M. G.; Maxwell, J. M.; Pearson, R. D.; Vuocolo, T.; Liyou, N. E.; Wong, D. C. C.; Merritt, D. J.; Dixon, N. E. *Nature* **2005**, *437* (7061), 999−1002.

(8) Li, L.; Teller, S.; Clifton, R. J.; Jia, X.; Kiick, K. L. *Biomacromolecules* **2011**, *12* (6), 2302−2310.

DOI: 10.1021/acs.biomac.7b00294
Biomacromolecules 2017, 18, 1866−1873

(9) Balu, R.; Knott, R.; Cowieson, N. P.; Elvin, C. M.; Hill, A. J.; Choudhury, N. R.; Dutta, N. K. *Sci. Rep.* **2015**, *5*, 10896−10908.
(10) Nairn, K. M.; Lyons, R. E.; Mulder, R. J.; Mudie, S. T.; Cookson, D. J.; Lesieur, E.; Kim, M.; Lau, D.; Scholes, F. H.; Elvin, C. M. *Biophys. J.* **2008**, *95* (7), 3358−3365.
(11) Qin, G.; Hu, X.; Cebe, P.; Kaplan, D. L. *Nat. Commun.* **2012**, *3*, 1003−1011.
(12) Dutta, N. K.; Truong, M. Y.; Mayavan, S.; Roy Choudhury, N.; Elvin, C. M.; Kim, M.; Knott, R.; Nairn, K. M.; Hill, A. J. *Angew. Chem., Int. Ed.* **2011**, *50* (19), 4428−4431.
(13) Li, L.; Kiick, K. L. *ACS Macro Lett.* **2013**, *2* (8), 635−640.
(14) Truong, M. Y.; Dutta, N. K.; Choudhury, N. R.; Kim, M.; Elvin, C. M.; Hill, A. J.; Thierry, B.; Vasilev, K. *Biomaterials* **2010**, *31* (15), 4434−4446.
(15) Palonen, H.; Tenkanen, M.; Linder, M. *Appl. Environ. Microbiol.* **1999**, *65* (12), 5229−5233.
(16) Bayer, E. A.; Morag, E.; Lamed, R. *Trends Biotechnol.* **1994**, *12*, 379−386.
(17) Várnai, A.; Mäkelä, M. R.; Djajadi, D. T.; Rahikainen, J.; Hatakka, A.; Viikari, L. *Adv. Appl. Microbiol.* **2014**, *88*, 103−165.
(18) Fang, W.; Arola, S.; Malho, J.; Kontturi, E.; Linder, M. B. *Biomacromolecules* **2016**, *17* (4), 1458−1465.
(19) Rivkin, A.; Abitbol, T.; Nevo, Y.; Verker, R.; Lapidot, S.; Komarov, A.; Veldhuis, S. C.; Zilberman, G.; Reches, M.; Cranston, E. D.; Shoseyov, O. *Ind. Biotechnol.* **2015**, *11*, 44−58.
(20) Swerin, A.; Odberg, L.; Lindstrbm, T.; Pulp, S. *Nord. Pulp Pap. Res. J.* **1990**, *5* (4), 188−196.
(21) Landowski, C. P.; Mustalahti, E.; Wahl, R.; Croute, L.; Sivasiddarthan, D.; Westerholm-Parvinen, A.; Sommer, B.; Ostermeier, C.; Helk, B.; Saarinen, J.; Saloheimo, M. *Microb. Cell Fact.* **2016**, *15*, 104.
(22) Sarrion-Perdigones, A.; Falconi, E. E.; Zandalinas, S. I.; Juarez, P.; Fernandez-del-Carmen, A.; Granell, A.; Orzaez, D. *PLoS One* **2011**, *6* (7), e21622.
(23) Colot, H. V.; Park, G.; Turner, G. E.; Ringelberg, C.; Crew, C. M.; Litvinkova, L.; Weiss, R. L.; Borkovich, K. A.; Dunlap, J. C. *Proc. Natl. Acad. Sci. U. S. A.* **2006**, *103* (27), 10352−10357.
(24) Landowski, C. P.; Huuskonen, A.; Wahl, R.; Westerholm-Parvinen, A.; Kanerva, A.; Hänninen, A. L.; Salovuori, N.; Penttilä, M.; Natunen, J.; Ostermeier, C.; Helk, B.; Saarinen, J.; Saloheimo, M. *PLoS One* **2015**, *10* (8), e0134723.
(25) Penttilä, M.; Nevalainen, H.; Rättö, M.; Salminen, E.; Knowles, J. *Gene* **1987**, *61* (2), 155−164.
(26) Malho, J. M.; Arola, S.; Laaksonen, P.; Szilvay, G. R.; Ikkala, O.; Linder, M. B. *Angew. Chem., Int. Ed.* **2015**, *54* (41), 12025−12028.
(27) Arola, S.; Linder, M. B. *Sci. Rep.* **2016**, *6*, 35358−35367.
(28) Bochicchio, B.; Pepe, A.; Tamburro, A. M. *Chirality* **2008**, *20*, 985−994.
(29) Adzhubei, A. A.; Sternberg, M. J. E.; Makarov, A. A. *J. Mol. Biol.* **2013**, *425*, 2100−2132.
(30) Lopes, J. L. S.; Miles, A. J.; Whitmore, L.; Wallace, B. A. *Protein Sci.* **2014**, *23* (12), 1765−1772.
(31) Mautner, A.; Maples, H. A.; Sehaqui, H.; Zimmermann, T.; de Larraya, U.; Mathew, A. P.; Lai, C. Y.; Li, K.; Bismarck, A. *Environ. Sci. Res. Technol.* **2016**, *2* (1), 117−124.
(32) Linder, M.; Nevanen, T.; Soderholm, L.; Bengs, O.; Teeri, T. T. *Biotechnol. Bioeng.* **1998**, *60* (5), 642−647.
(33) Carrard, G.; Linder, M. *Eur. J. Biochem.* **1999**, *262* (3), 637−643.
(34) Linder, M.; Salovuori, I.; Ruohonen, L.; Teeri, T. T. *J. Biol. Chem.* **1996**, *271* (35), 21268−21272.
(35) Malho, J. M.; Ouellet-Plamondon, C.; Rüggeberg, M.; Laaksonen, P.; Ikkala, O.; Burgert, I.; Linder, M. B. *Biomacromolecules* **2015**, *16* (1), 311−318.
(36) Truong, M. Y.; Dutta, N. K.; Choudhury, N. R.; Kim, M.; Elvin, C. M.; Nairn, K. M.; Hill, A. J. *Biomaterials* **2011**, *32* (33), 8462−8473.

DOI: 10.1021/acs.biomac.7b00294
Biomacromolecules 2017, 18, 1866−1873